J. Fluid Mech. (1993), *vol.* 252, *pp.* 187–207

Simple shear flow of a suspension of fibres in a dilute polymer solution at high Deborah number

By O. G. HARLEN[1] AND DONALD L. KOCH[2]

[1] Department of Applied Mathematics and Theoretical Physics, University of Cambridge, Silver Street, Cambridge, CB3 9EW, UK

[2] School of Chemical Engineering, Cornell University, Ithaca, NY 14853, USA

(Received 26 June 1992 and in revised form 11 January 1993)

The behaviour of fibre suspensions in dilute polymer solutions at high Deborah numbers is analysed. In particular, we calculate the change to the extension of the polymers and the orientation of the fibres caused by hydrodynamic interactions between the polymers and the fibres. At a sufficiently high Deborah number the combined effect of the fibre velocity disturbances and the mean shear flow produce a dramatic increase in the extension of the polymers, similar to the coil–stretch transition observed in extensional flow.

The non-Newtonian stresses caused by the polymers produce a perturbation to the angular velocity of the fibres, giving rise to a net drift across Jeffery orbits towards the vorticity axis. Unlike the second-order-fluid analysis of Leal (1975), this effect does not depend on the second-normal-stress difference.

1. Introduction

The shear-flow behaviour of fibre suspensions in Newtonian fluids has been an active area of research dating back to Jeffery's (1922) calculation of the orbit of an ellipsoidal particle in a linear flow. However, in many practical applications, such as injection moulding, the suspending fluid is viscoelastic. In this paper we investigate the case when the suspending fluid is a dilute polymer solution at shear rates which are large compared to the relaxation rate of the polymer (i.e. high Deborah numbers).

At high Deborah numbers the addition of small amounts of polymer to a Newtonian fluid can produce a large increase in the viscosity measured in an extensional flow. However, in simple shear flow the increase in viscosity is very much smaller. Similarly, the addition of fibres to a Newtonian fluid produces a much smaller increase in the shear viscosity compared to the increase in extensional viscosity of the suspension. A question arises as to what happens to the shear viscosity of a mixture of both fibres and polymers. If the fibres and polymers behave independently then we would expect only a small change in the viscosity of the suspension. On the other hand, it is possible that there may be interactions between the fibres and the polymers which give rise to a much larger increase in viscosity.

In an extensional flow the polymers stretch parallel to the extensional axis, so that the velocity difference across the molecule, and consequently the stretching force, increase as it extends. By contrast, in shear flow the polymer molecules stretch in the flow direction, perpendicular to the velocity gradient, and so the velocity difference across a molecule remains small. In a fibre suspension the polymers no longer experience purely simple shear flow, because of disturbances produced by the fibres. If the effect of these disturbances is to rotate the polymers away from alignment with the

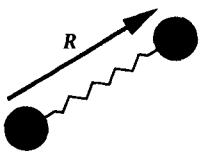

FIGURE 1. Sketch of an elastic dumbbell.

flow direction, then the shear flow can stretch them further. In §2 we use the method of averaged equations to calculate the average extension of a polymer molecule in a random suspension of fibres undergoing simple shear.

The analysis is based on the method used by Shaqfeh & Koch (1988*a*, *b*) to study the alignment of an axisymmetric particle flowing through a random fixed bed. Their predictions of particle orientations have been verified by light scattering measurements (Frattini *et al.* 1991). In a recent paper, Shaqfeh & Koch (1992), applied this technique to polymer solutions flowing through a random fixed bed of fibres or spheres. Above a critical flow rate, the polymers become highly extended, causing an increase in the resistance to flow. Experimental measurements of flow through fixed beds (e.g. James & MacClaren 1975) find a significant increase in flow resistance when a small concentration of polymer is added to a Newtonian fluid.

The orientation of an isolated fibre in Newtonian fluid follows one of a family of closed curves called Jeffery orbits (Jeffery 1922), depending on its initial orientation. The distribution of a suspension of fibres between different Jeffery orbits cannot be found from the motion of an isolated fibre, but depends on secondary effects such as interactions between fibres. In the case of a weakly non-Newtonian fluid, the non-Newtonian stresses are expected to perturb the Jeffery rotation and may cause the fibres to drift between Jeffery orbits. Experimental observations of the motion of fibres in polymer solutions (Bartram, Goldsmith & Mason 1975) find that the fibres in general drift towards an alignment parallel the vorticity axis. For low Deborah numbers, Leal (1975) calculated the perturbation to Jeffery orbits for a second-order fluid. His analysis predicts a drift towards the vorticity axis for fluids with a second-normal-stress difference, in qualitative agreement with experiment. However, Iso, Koch & Cohen (1993) observe that fibres also drift towards the vorticity axis in polyisobutylene Boger fluids (Boger 1977), which have zero second-normal-stress differences (Magda *et al.* 1991). In §3 we show that at high Deborah numbers fibres drift towards the vorticity axis due to a mechanism which is independent of the second-normal-stress difference.

Throughout this paper n denotes the number density of fibres and l the fibre half-length. The fibre aspect ratio r, is assumed to be large so that results of slender-body theory (Batchelor 1970) can be used. Our analysis is performed first for the dilute limit ($nl^3 \ll 1$), and then extended to semi-dilute suspensions ($1 \ll nl^3 \ll r$) in §2.6. The extension to semi-dilute is important because it is in this limit that the largest effect on the polymer stress is to be found.

Cartesian coordinates (x, y, z) are defined such that 1 (or $\hat{x}$) is flow direction, 2 the gradient direction and 3 the axis of vorticity, and in these coordinates the unperturbed shear flow is given by

$$\boldsymbol{u}^* = (\gamma y, 0, 0). \tag{1}$$

2. Polymer conformation

2.1. *Polymer model*

The distortion of a polymer molecule by the flow is modelled as the extension of an elastic dumbbell consisting of two beads joined by an elastic spring (Kuhn & Kuhn 1945). This represents the gross distortion of the molecule in terms of a single vector $\boldsymbol{R}^*$ (see figure 1), the bead separation. The simplest model employs a linear (Hookean) spring and constant hydrodynamic friction, for which the evolution of $\boldsymbol{R}^*$ is given by

$$\frac{\mathrm{d}\boldsymbol{R}^*}{\mathrm{d}t} \equiv \dot{\boldsymbol{R}}^* = \boldsymbol{R}^* \cdot \boldsymbol{\nabla}^* \boldsymbol{u}^* - \kappa \boldsymbol{R}^*, \tag{2}$$

where κ is the relaxation rate of the polymer. The probability distribution $P(\boldsymbol{x}^*, \boldsymbol{R}^*)$ obeys the conservation equation

$$\frac{\partial P}{\partial t^*} + \boldsymbol{u}^* \cdot \boldsymbol{\nabla}^* P + \boldsymbol{\nabla}_{\boldsymbol{R}^*} \cdot (\dot{\boldsymbol{R}}^* P) - 2D_m \nabla^2_{\boldsymbol{R}^*} P = 0, \tag{3}$$

where D_m is the bead diffusivity. Here we assume that the Péclet number is large so that diffusion of the dumbbell's centre of mass can be neglected.

At this point it is useful to introduce dimensionless variables by scaling lengths with the fibre half-length, l, and time derivatives with the shear-rate γ. The polymer extension $\boldsymbol{R}$ is scaled on its equilibrium value in zero flow so that

$$\boldsymbol{R}^* = \boldsymbol{R}(2D_m/\kappa)^{\frac{1}{2}}, \quad \boldsymbol{x}^* = \boldsymbol{x}l, \quad \text{and} \quad t^* = \gamma^{-1} t. \tag{4}$$

The Deborah number, D is defined to be

$$D = \gamma/\kappa. \tag{5}$$

In dimensionless variables (2) becomes

$$\dot{\boldsymbol{R}} = \boldsymbol{R} \cdot \boldsymbol{\nabla} \boldsymbol{u} - (1/D)\, \boldsymbol{R}. \tag{6}$$

This model has the correct behaviour for small distortions, but behaves unphysically in extensional flows with $D > 1$ (see Rallison & Hinch 1988). This can be remedied by using a finitely extensible nonlinear elastic (FENE) spring law (Warner 1972), which prevents the dumbbell from extending beyond a maximum length R_{m}. For this model $1/D$ in (6) is replaced by the $f(|\boldsymbol{R}|)/D$ where

$$f(R) = \frac{1}{1 - R^2/R_{\mathrm{m}}^2}. \tag{7}$$

In the following subsection we will develop the theory using the linear model and discuss the modifications for the FENE model in §2.4.

2.2. *Polymers in a fibre suspension*

We now seek the average extension of a polymer in a dilute suspension of fibres undergoing simple shear flow. The polymer is assumed to be sufficiently dilute that it does not affect the dynamics. Therefore, strictly speaking our results are valid only for extremely low polymer concentrations when the solution is effectively Newtonian, but it is hoped that the results remain valid, at least qualitatively, at higher concentrations.

For a homogeneous suspension it suffices to determine the polymer conformation distribution at a single point in space. We define the joint probability density function for the extension of the polymer, $\boldsymbol{R}$, at the origin and the positions, $\boldsymbol{x}_i$, and orientations, $\boldsymbol{p}_i$, of the fibres to be

$$P(\boldsymbol{R}, \boldsymbol{x}_1, \boldsymbol{p}_1, \ldots, \boldsymbol{x}_N, \boldsymbol{p}_N, t),$$

which satisfies the conservation equation

$$\frac{\partial P}{\partial t}+\sum_{i=1}^{N}[\nabla_{x_i}\cdot(\dot{x}_i P)+\nabla_{p_i}\cdot(\dot{p}_i P)]+\nabla_R\cdot(\dot{R}P)-\frac{1}{D}\nabla_R^2 P=0. \tag{8}$$

We will use two different forms of ensemble average; the first, denoted by $\langle\ \rangle_0$,

$$\langle Q\rangle_0 \equiv \int\left(\prod_{i=1}^{N} \mathrm{d}^3\boldsymbol{x}_i\,\mathrm{d}^2\boldsymbol{p}_i\right) QP(\boldsymbol{R},\boldsymbol{x}_1,\boldsymbol{p}_1,\ldots,t), \tag{9}$$

is the average over positions and orientations of all of the fibres; and $\langle\ \rangle_1$

$$\langle Q\rangle_1 \equiv \int\left(\prod_{i=2}^{N} \mathrm{d}^3\boldsymbol{x}_i\,\mathrm{d}^2\boldsymbol{p}_i\right) QP(\boldsymbol{R},\boldsymbol{x}_1,\boldsymbol{p}_1,\ldots,t), \tag{10}$$

represents the conditional average with a fibre at position $\boldsymbol{x}$ and orientation $\boldsymbol{p}$.

In order to proceed with the analysis we need to make a number of simplifying assumptions. First, the disturbance caused by the entire suspension of fibres is approximated as the sum of disturbances caused by each individual fibre in the absence of the other fibres (i.e. we neglect fibre–fibre interactions). This approximation involves errors of order $(nl^3)^2$. Second, we assume that the dominant contribution of the fibres to the mean extension of the polymer comes from fibres at distances of the order of a fibre length from the polymer. Each interaction causes only a small disturbance to the flow at the origin of order $1/\log(r)$, but the combined effect of a large number of such interactions has a significant effect on the extension of the polymer. A fibre which passes within a fibre radius of the polymer will produce a large disturbance, and may cause a large extension of the polymer in a single interaction. However, the probability that a fibre will pass that close to the origin is nl^3/r^2 which is negligible for fibres of high aspect ratio. Furthermore, in the neighbourhood of a fibre the relative flow is parallel to the fibre and so the effect of close interactions is less important here than in the case of a fixed bed considered by Shaqfeh & Koch (1992). Third, we assume that the Deborah number is large so that the relaxation of the polymer can be ignored during an interaction with a fibre. However, the effect of relaxation between interactions is included.

It is convenient to express the velocity $\boldsymbol{u}$ as

$$\boldsymbol{u}=\boldsymbol{u}_0+\boldsymbol{u}^{\mathrm{f}}, \tag{11}$$

where $\boldsymbol{u}_0=(y,0,0)$ is the unperturbed shear flow and $\boldsymbol{u}^{\mathrm{f}}$ is the perturbation caused by the fibres, which is smaller by a factor of $1/\log(r)$ than the mean flow. Since $\boldsymbol{u}^{\mathrm{f}}$ is small, at leading order the joint probability density function, P, will be equal to the uncorrelated distribution for the polymer and the fibres,

$$P_{\mathrm{U}}=\Omega(\boldsymbol{R})\prod_{i=1}^{N}\frac{l^3}{V}g(\boldsymbol{p}_i), \tag{12}$$

where $\Omega(\boldsymbol{R})\equiv\langle P\rangle_0$ is the probability distribution for the extension of the polymer and $g(\boldsymbol{p})$ is the orientation distribution of a fibre in shear flow.

For a dilute suspension of fibres the leading-order contribution to the correlated distribution comes from correlations between a single fibre and the polymer. Thus we may approximate $P'\equiv P-P_{\mathrm{U}}$ in the form

$$P'=\sum_{i=1}^{N}\frac{l^3}{V}\Omega_1(\boldsymbol{R},\boldsymbol{x}_i,\boldsymbol{p}_i)\prod_{j=1,j\neq i}^{N}\frac{l^3}{V}g(\boldsymbol{p}_j), \tag{13}$$

where $(l^3/V)\,\Omega(\boldsymbol{R})\,g(\boldsymbol{p})+\Omega_1(\boldsymbol{R},\boldsymbol{x},\boldsymbol{p}) \equiv \langle P\rangle_1$ is the joint probability density for a fibre and a polymer. This expression for P' neglects correlations involving more than one fibre which are of order nl^3 smaller.

Integrating (8) over $\boldsymbol{x}_i$ and $\boldsymbol{p}_i$, and using the expression for P given by (12) and (13), we obtain

$$\frac{\partial\Omega}{\partial t}-\frac{1}{D}[\nabla_R\cdot(R\Omega)+\nabla_R^2\Omega]+\nabla_R\cdot(\boldsymbol{R}\cdot\nabla\langle\boldsymbol{u}\rangle_0\,\Omega)$$

$$=-nl^3\,\nabla_R\cdot\left(\boldsymbol{R}\cdot\int d^3x\,d^2p\,\nabla\langle\boldsymbol{u}^f\rangle_1\,\Omega_1\right). \quad (14)$$

To close this system we need a second equation for Ω_1, which is obtained by taking the one-particle conditional average of (8) and subtracting $nl^3 g(\boldsymbol{p})\times$ equation (14), which yields

$$\frac{\partial\Omega_1}{\partial t}+\nabla\cdot(\langle\boldsymbol{u}\rangle_0\,\Omega_1)+\nabla_p\cdot(\langle\dot{\boldsymbol{p}}\rangle_0\,\Omega_1)-\frac{1}{D}[\nabla_R\cdot(R\Omega_1)+\nabla_R^2\Omega_1]$$

$$+\nabla_R\cdot(\boldsymbol{R}\cdot\nabla\langle\boldsymbol{u}\rangle_0\,\Omega_1)=-g(\boldsymbol{p})\,\nabla_R\cdot(\boldsymbol{R}\cdot\nabla\langle\boldsymbol{u}^f\rangle_1\,\Omega). \quad (15)$$

Since the velocity disturbance $\boldsymbol{u}^f$ is small compared to the shear flow, the average rotation rate of the fibre $\langle\dot{\boldsymbol{p}}\rangle_0$ is equal to the Jeffery rotation rate at this approximation.

The time taken for the fibre to pass the polymer is of order unity, and so the change in the extension of the polymer caused by a single interaction is of order $1/\log(r)$. The terms

$$(1/D)[\nabla_R\cdot(R\Omega_1)+\nabla_R^2\Omega_1]$$

correspond to the relaxation of the polymer during the time of the interaction and may be neglected provided that $D\gg\log(r)$.

The term

$$\nabla_R\cdot(\boldsymbol{R}\cdot\nabla\langle\boldsymbol{u}\rangle_0\,\Omega_1)=R_2\,\partial\Omega_1/\partial R_1$$

represents the stretching of the polymer by the shear flow. During the time of an interaction, the shear flow changes R_1 by an amount of order R_2. We shall see later that R_2 is or order $1/D$ smaller than R_1 and so the relative change is only of order $1/D$. Thus this term may also be neglected for $D\gg\log(r)$.

Thus in the limit when $D\gg\log(r)$ the steady-state value of Ω_1 satisfies

$$y\,\partial\Omega_1/\partial x+\nabla_p\cdot(\dot{\boldsymbol{p}}\Omega_1)=-g(\boldsymbol{p})\,\nabla_R\cdot(\boldsymbol{R}\cdot\nabla\langle\boldsymbol{u}^f\rangle_1\,\Omega)+O(nl^3,\log(r)/D). \quad (16)$$

The terms on the left-hand side of (16) represents convection of the disturbance Ω_1 along a fibre trajectory, and can be rewritten in the form

$$\frac{y}{\omega(\boldsymbol{p}(s))}\frac{d}{ds}(\omega(\boldsymbol{p}(s))\,\Omega_1), \quad (17)$$

where s is the x-coordinate of the fibre position along the trajectory, and the integrating factor, ω, is given by

$$\omega=\int ds\,\nabla_p\cdot\dot{\boldsymbol{p}}. \quad (18)$$

Integrating along a fibre trajectory, we find

$$\Omega_1=-\frac{1}{y\omega(\boldsymbol{p})}\int_{-\infty\,\mathrm{sgn}(y)}^{x} ds\,g[\boldsymbol{p}(s)]\,\omega[\boldsymbol{p}(s)]\,\nabla_R\cdot[\boldsymbol{R}\cdot\nabla\langle\boldsymbol{u}^f\rangle_1(\boldsymbol{x}(s),\boldsymbol{p}(s))\,\Omega]. \quad (19)$$

Substituting this expression of Ω_1 in (14) and noting from continuity that $\nabla \cdot \langle \boldsymbol{u}^{\mathrm{f}} \rangle_1 = 0$, we obtain

$$\frac{\partial \Omega}{\partial t} + \nabla_R \cdot (\boldsymbol{R} \cdot \nabla \langle \boldsymbol{u} \rangle_0 \Omega) - \frac{1}{D} \nabla_R \cdot (\boldsymbol{R}\Omega) + \nabla_R \cdot (\boldsymbol{d} \cdot \nabla_R \Omega) = 0, \tag{20}$$

where the anisotropic diffusivity $\boldsymbol{d}$ contains two terms: an isotropic term from the Brownian diffusion of the beads, and a second anisotropic term due to the fibres.

$$d_{ik} = (1/D)\,\delta_{ik} + nl^3 M_{ijkl} R_j R_l. \tag{21}$$

Here, we have used Einstein's suffix notation for clarity. The tensor M_{ijkl} is essentially a correlation of the velocity gradient perturbation along a fibre trajectory,

$$M_{ijkl} = \int \mathrm{d}^3\boldsymbol{x}\, \mathrm{d}^2\boldsymbol{p} \nabla_j \langle u_i^{\mathrm{f}} \rangle_1 \frac{1}{y\omega(\boldsymbol{p})} \int_{-\infty \mathrm{sgn}(y)}^{x} \mathrm{d}s\, \omega(\boldsymbol{p}(s))\, g(\boldsymbol{p}(s))\, \nabla_l \langle u_k^{\mathrm{f}} \rangle_1. \tag{22}$$

Equation (20) involves errors of order $(nl^3)^2$ and $(nl^3 \log(r)/D)$. Calculation of the tensor M_{ijkl} is left until §2.5. For a dilute suspension of fibres the largest contribution to the integral comes from the $1/r$ fraction of fibres which are at an angle of order unity from the flow–vorticity (1,3)-plane. The velocity disturbances produced by these fibres are of order $1/\log(r)$, and so M_{ijkl} will be of order $1/r\log^2(r)$.

We define $\boldsymbol{A}$ to be the second-moment tensor

$$\boldsymbol{A} \equiv \int \mathrm{d}^3\boldsymbol{R}\, P(\boldsymbol{R})\, \boldsymbol{RR}, \tag{23}$$

and taking the ensemble average

$$\langle \boldsymbol{A} \rangle_0 \equiv \int \mathrm{d}^3\boldsymbol{R}\, \Omega(\boldsymbol{R})\, \boldsymbol{RR}, \tag{24}$$

multiplying (20) by $\boldsymbol{RR}$ and integrating over $\boldsymbol{R}$, we obtain a closed equation for $\langle \boldsymbol{A} \rangle_0$. At steady state $\langle \boldsymbol{A} \rangle_0$ satisfies

$$\begin{aligned} &\langle A_{kj} \rangle_0 \partial_k \langle u_i \rangle_0 + \langle A_{ik} \rangle_0 \partial_k \langle u_j \rangle_0 - (2/D)(\langle A_{ij} \rangle_0 - \delta_{ij}) \\ &\quad = -nl^3[(M_{ikjm} + M_{jkim}) \langle A_{km} \rangle_0 + M_{kmik} \langle A_{mj} \rangle_0 + M_{kmjk} \langle A_{im} \rangle_0]. \end{aligned} \tag{25}$$

This set of six coupled linear equations could be solved for general D, but we will instead examine the limit of large D when the largest terms on the right-hand side are of order nl^3D^3. Neglecting smaller terms and noting that $\langle \boldsymbol{u} \rangle_0 = \boldsymbol{u}_0$, the 11, 12 and 22 components of (25) are respectively

$$\left.\begin{aligned} D\langle A_{12} \rangle_0 - \langle A_{11} \rangle_0 + 1 &\approx 0, \\ D\langle A_{22} \rangle_0 - 2\langle A_{12} \rangle_0 &\approx 0, \\ -\langle A_{22} \rangle_0 + 1 &\approx -Dnl^3 M_{2121} \langle A_{11} \rangle_0, \end{aligned}\right\} \tag{26}$$

with solution

$$\langle A_{11} \rangle_0 \approx \frac{D^2}{2 - D^3 nl^3 M_{2121}}, \quad \langle A_{12} \rangle_0 \approx \frac{D}{2 - D^3 nl^3 M_{2121}}, \quad \langle A_{22} \rangle_0 \approx \frac{2}{2 - D^3 nl^3 M_{2121}}. \tag{27}$$

(For a dilute suspension of fibres we will find (equation (51)), that $M_{2121} = 0.038/r\log^2(r)$.)

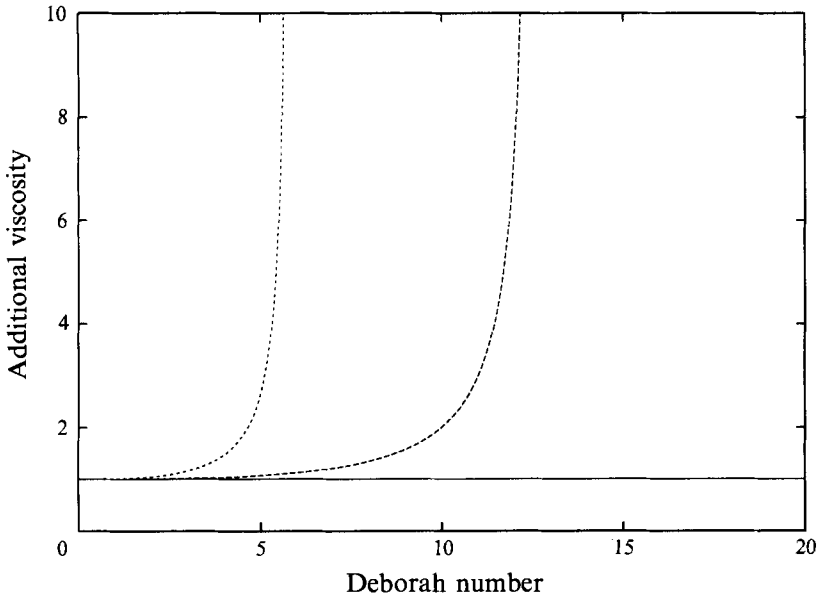

FIGURE 2. The polymer contribution to the shear viscosity, $2\langle A_{12}\rangle_0/D$, as a function of Deborah number at various fibre concentrations: ——, $nl^3 = 0$; – – –, $nl^3M_{2121} = 0.001$; ....., $nl^3M_{2121} = 0.01$.

The average stress within the suspension is equal to the sum of the solvent stress and the stresses exerted by the fibres and the polymers. The contribution from the fibres is of order nl^3/r times the solvent stress and is, therefore, negligible. For a concentration of n_p dumbbells per unit volume of bead radius R_g, the polymeric stress is given by

$$\boldsymbol{\sigma}^p = (2c/D)\langle \boldsymbol{A}\rangle_0, \tag{28}$$

where $c = n_p \pi R_g^3$ is a measure of the volume concentration of dumbbells. The effective shear viscosity of the suspension is therefore given by

$$\mu_{\text{shear}} = 1 + (2c/D)\langle A_{12}\rangle_0.$$

In the absence of fibres $\langle A_{12}\rangle_0/D$ is equal to 0.5, and so the shear viscosity is constant. With the addition of fibres, the viscosity increases with Deborah number as

$$\mu_{\text{shear}} = 1 + \frac{2c}{2 - D^3nl^3M_{2121}}. \tag{29}$$

This increase is illustrated in figure 2 which shows the variation in the polymer contribution to the shear viscosity, $2\langle A_{12}\rangle_0/D\,(= (\mu_{\text{shear}} - 1)/c)$, with Deborah number.

The first- and second-normal-stress differences are respectively

$$c(\langle A_{11}\rangle_0 - \langle A_{22}\rangle_0) = \frac{cD^2}{2 - D^3nl^3M_{2121}},$$

$$c(\langle A_{22}\rangle_0 - \langle A_{33}\rangle_0) = \frac{cD^3nl^3(M_{2121} - M_{3131})}{2 - D^3nl^3M_{2121}}.$$

At a critical Deborah number of

$$D_{\text{crit}} = (2/nl^3M_{2121})^{\frac{1}{3}}$$

the dumbbells become infinitely extended and the viscosity and normal stresses become

infinite. Although this behaviour is obviously unrealistic and may be corrected by changing to an FENE dumbbell model (see §2.4), the critical Deborah number marks the transition of the polymer from a coiled to a highly extended configuration, and corresponds to the onset of strongly non-Newtonian behaviour. For a dilute suspension of fibres the critical Deborah number is

$$D_{\text{crit}} = 3.7 \times \left(\frac{nl^3}{r \log^2 r}\right)^{-\frac{1}{3}},$$

and will in practice be quite large, since $nl^3/r \ll 1$.

The above results are for steady state, but we can also estimate the time required for unextended polymers to become extended. In a pure shear flow, fluid elements separate algebraically in time and so the extension of the dumbbell increases approximately linearly with time. In a sheared fibre suspension, the time-dependent version of (26) is

$$\left.\begin{aligned} \frac{\partial \langle A_{11}\rangle_0}{\partial t} - 2\langle A_{12}\rangle_0 + \frac{2}{D}(\langle A_{11}\rangle_0 - 1) &\approx 0, \\ \frac{\partial \langle A_{12}\rangle_0}{\partial t} - \langle A_{22}\rangle_0 + \frac{2}{D}\langle A_{12}\rangle_0 &\approx 0, \\ \frac{\partial \langle A_{22}\rangle_0}{\partial t} + \frac{2}{D}(\langle A_{22}\rangle_0 - 1) &\approx 2nl^3 M_{2121}\langle A_{11}\rangle_0. \end{aligned}\right\} \tag{30}$$

At high Deborah numbers we may neglect terms of order $1/D$, in which case $\langle A_{11}\rangle_0$ increases exponentially in time as

$$\langle A_{11}\rangle_0 = \exp\left[(4nl^3 M_{2121})^{\frac{1}{3}}\, t\right]. \tag{31}$$

Hence, the dumbbells stretch in a time of order D_{crit}/γ.

2.3. *Physical mechanism*

A coil–stretch transition of this kind occurs in the absence of fibres in linear flows where the extension rate is greater than the rate of rotation, but not in simple shear flow. Simple shear is the special case where the extension rate and rotation rate are equal, and the rotation is just sufficient to prevent the extensional component of the flow from stretching the polymer. The velocity perturbations caused by the fibres affect this balance between extension and rotation in such a way that the extensional component of the flow is able to produce a catastrophic increase in the extension of the dumbbell.

For flow through a fixed bed, Shaqfeh & Koch (1992) show that the velocity disturbances caused by the fibres produce a coil–stretch transition at a critical Deborah number dependent on the fibre density. The mean flow through the bed is uniform and so it does not contribute to the extension of the dumbbells, but merely convects them through the bed. Conversely, in a sheared suspension of fibres the mean shear flow has an extensional component and so it is possible for there to be a coupling between the fibre disturbance velocity and the mean flow.

To see how this coupling works, consider a single interaction between a fibre and a dumbbell which is initially extended in the flow direction, as sketched schematically in figure 3. As the fibre moves past the dumbbell, the velocity disturbance created by the fibre deflects the ends of the dumbbell from their original streamlines. The fibre rotates as it passes the dumbbell and so the two ends of the dumbbell experience a slightly

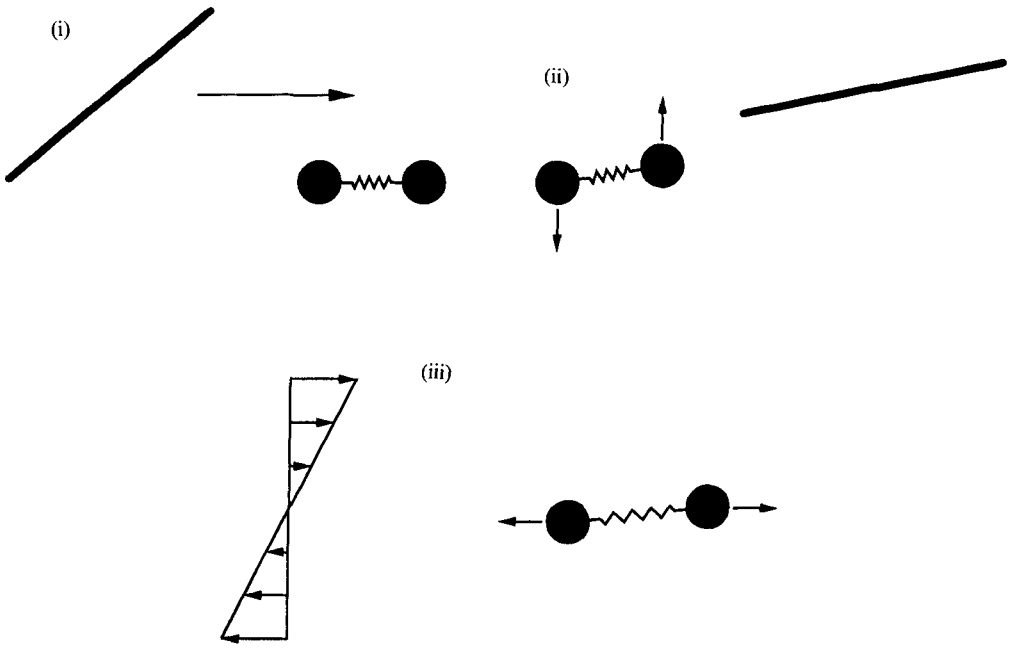

FIGURE 3. Sketch of the mechanism for stretching the dumbbell. (i, ii) The velocity disturbance caused by a passing fibre rotates the dumbbell in the gradient direction. (iii) The rotated dumbbell is stretched in the flow direction by the shear flow.

different flow history, and in general will be displaced by different amounts from their original streamlines. Thus a dumbbell which was initially aligned parallel to the flow direction is rotated slightly in the gradient direction. The breaking of the flow symmetry by the rotation of the fibre is crucial to this rotation of the dumbbell, and would not occur for a suspension of spheres.

As a result of the interaction, the two ends of the dumbbell now lie on different streamlines and consequently the mean shear flow will stretch the dumbbell in the flow direction. Thus the initial extension in the flow direction has been enhanced via a small rotation in the gradient direction caused by the fibre, which enables the shear flow to stretch the dumbbell.

It is therefore the mean shear flow rather than the fibre velocity disturbance which is primarily responsible for stretching the dumbbells, in contrast to the case of flow through a fixed bed where the flow perturbations are responsible for stretching the dumbbells (Shaqfeh & Koch 1992). The most important effect of the additional bead diffusion is the relative diffusion of the ends of the dumbbell in the gradient direction. Consequently, it is the 22-component of $\boldsymbol{d}$ which appears in the solution for $\langle A_{11}\rangle_0$.

Between interactions the dumbbells will try to relax back to their equilibrium conformations. However, for a sufficiently large fibre concentration, the frequency of interactions will be too high for the dumbbells to have sufficient time to relax before the next interaction with a fibre. The feedback mechanism outlined above will then cause an infinite extension unless prevented by a nonlinear spring.

2.4. *FENE dumbbells*

For the linear dumbbell model, there are no steady solutions for $\langle \boldsymbol{A}\rangle_0$ at Deborah numbers above D_{crit}. This singular behaviour also occurs in extensional flows and may be remedied by changing to a nonlinear spring which prevents the dumbbells from

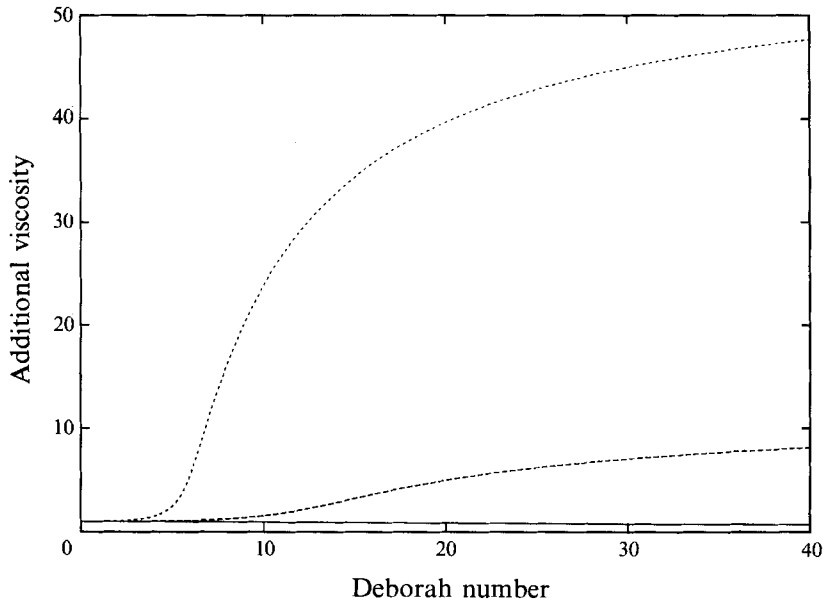

FIGURE 4. The polymer contribution to the shear viscosity, $2f\langle A_{12}\rangle_0/D$, for FENE dumbbells with $R_m = 30$ as a function of Deborah number at various fibre concentrations: ——, $nl^3 = 0$; – – –, $nl^3 M_{2121} = 0.001$; ....., $nl^3 M_{2121} = 0.01$.

extending beyond a finite limit. The change from linear to FENE dumbbells does not affect the averaging over configurations, because the relative velocity of the beads due to the spring force does not depend on the fibre configuration and the relaxation of the dumbbell is neglected during the interaction with a fibre. Thus the only change to (20) is to replace $1/D$ with $f(R)/D$. However, with this change it is no longer possible to form an exact closed equation for the second moment, $\langle \boldsymbol{A} \rangle_0$. To close this system we use the closure approximation introduced by Peterlin (1966) in which the nonlinear function $f(R)$ in (7) is approximated by $f(\mathrm{Tr}A)^{\frac{1}{2}}$. With this approximation the second-moment equations become

$$\left.\begin{aligned} D\langle A_{12}\rangle_0 - f\langle A_{11}\rangle_0 + 1 &\approx 0, \\ D\langle A_{22}\rangle_0 - 2f\langle A_{12}\rangle_0 &\approx 0, \\ -f\langle A_{22}\rangle_0 + 1 &\approx -Dnl^3 M_{2121}\langle A_{11}\rangle_0, \\ -f\langle A_{33}\rangle_0 + 1 &\approx -Dnl^3 M_{3131}\langle A_{11}\rangle_0. \end{aligned}\right\} \tag{32}$$

In the limit when R_m is large, f is approximately unity except when $\langle A_{11}\rangle_0 \gg \langle A_{22}\rangle_0$, or $\langle A_{33}\rangle_0$, and consequently f may be approximated by

$$f = \frac{R_m^2}{R_m^2 - \langle A_{11}\rangle_0}. \tag{33}$$

With this approximation f is the root of the quartic equation

$$2R_m^2 f^4 - 2R_m^2 f^3 - D^2(1 + nl^3 M_{2121} DR_m^2) f + nl^3 M_{2121} D^3 R_m^2 = 0, \tag{34}$$

with $f > 1$.

The shear viscosity of a solution of FENE dumbbells is given by

$$\mu_{\mathrm{shear}} = 1 + (2cf/D)\langle A_{12}\rangle_0.$$

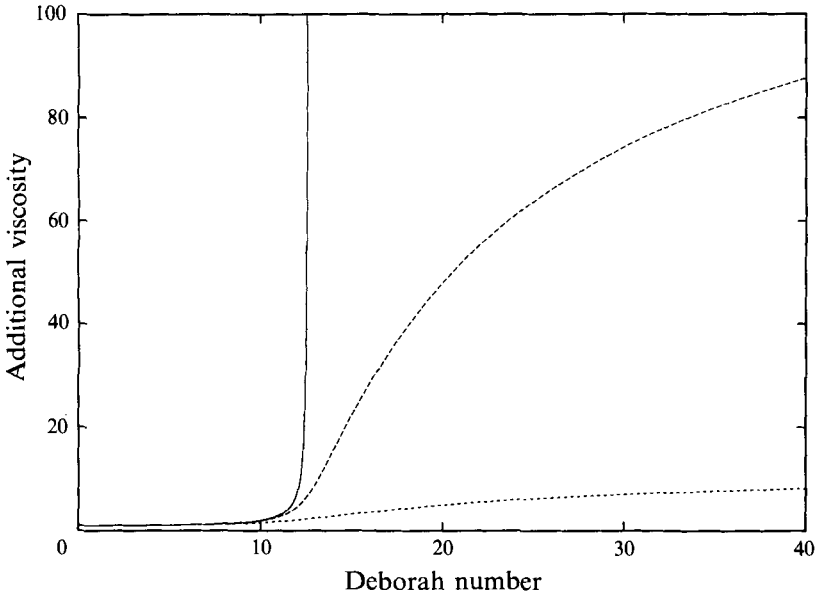

FIGURE 5. The polymer contribution to the shear viscosity, $2f\langle A_{12}\rangle_0/D$, as a function of Deborah number for different values of R_m with $nl^3M_{2121} = 0.001$: ——, $R_m = \infty$; – – –, $R_m = 100$; ....., $R_m = 30$.

In the absence of fibres $2f\langle A_{12}\rangle_0/D$ decreases with Deborah number, so the solution is weakly shear-thinning. With the addition of fibres, however, it increases with Deborah number, as shown in figure 4 (for $R_m = 30$). The effect of varying R_m is shown in figure 5. For finite values of R_m the shear viscosity does not become infinite, but asymptotes to a constant value of

$$\mu_{\text{shear}} \sim 1 + 2^{\frac{1}{3}} c R_m^2 (nl^3 M_{2121})^{\frac{2}{3}} \tag{35}$$

at high Deborah numbers. In deriving this expression for the limiting viscosity the hydrodynamic stress exerted by the polymer is calculated from the drag on the beads. In extensional flow this method produces an incorrect scaling for the limiting viscosity as a function of R_m. In this limit, the polymers are extended to their maximum length, and so behave like rigid fibres of length R_m. This provides an alternative expression for the limiting viscosity as

$$\mu_{\text{shear}} \sim 1 + \frac{2^{\frac{1}{3}} c R_m^3}{3 \log (R_m)} (nl^3 M_{2121})^{\frac{2}{3}}. \tag{36}$$

This predicts an increase in viscosity proportional to R_m^3 rather than R_m^2, giving a larger value of the limiting viscosity than equation (35).

2.5. M_{ijkl} *for a dilute fibre suspension*

In the previous subsections we derived the scaling for the extra diffusivity produced by the fibres and discussed its implications for the extension of the polymer. However, we did not calculate the values of the components of the tensor M_{ijkl}. From (22), M_{ijkl} is given by

$$M_{ijkl} = \int \mathrm{d}^3\boldsymbol{x}\, \mathrm{d}^2\boldsymbol{p} \langle \nabla_j u_i^f \rangle_1 \frac{1}{y\omega(\boldsymbol{p})} \int_{-\infty \operatorname{sgn}(y)}^{x} \mathrm{d}s \omega(\boldsymbol{p}(s))\, g(\boldsymbol{p}(s))\, \langle \nabla_l u_k^f \rangle_1.$$

It proves easier to evaluate this integral in Fourier space, and by taking the transform of (20) and applying the product theorem we obtain

$$M_{ijkl} = \frac{1}{8\pi^3}\int \mathrm{d}^3\boldsymbol{k}\,\mathrm{d}^2\boldsymbol{p}\,\frac{(-k_j)\,\hat{u}_i(-\boldsymbol{k})}{k_1\,\hat{\omega}(\boldsymbol{p})}\int_{\infty\mathrm{sgn}(k_1)}^{k_2}\mathrm{d}\zeta\, g(\boldsymbol{p})\,\hat{\omega}(\boldsymbol{p})\,k_l\,\hat{u}_k, \tag{37}$$

where $\hat{\boldsymbol{u}}$ is the transform of the velocity disturbance, defined by

$$\hat{\boldsymbol{u}} = \int \mathrm{d}^3\boldsymbol{x}\,\mathrm{e}^{-\mathrm{i}\boldsymbol{k}\cdot\boldsymbol{x}}\langle \boldsymbol{u}_{\mathrm{f}}\rangle_1, \tag{38}$$

and the ζ-integration is along a streamline in Fourier space. In Fourier space the streamlines of the shear flow are lines of constant k_1 and k_3. For $k_1 > 0$ the direction of motion is towards negative k_2 and for $k_1 < 0$ towards positive k_2. Therefore, the ζ-integration is from $\infty\mathrm{sgn}(k_1)$ to k_2. The integrating factor $\hat{\omega}$ is now given by

$$\mathrm{d}\hat{\omega}/\mathrm{d}\zeta = \nabla_p\cdot\dot{\boldsymbol{p}}. \tag{39}$$

To proceed further we need expressions for the velocity disturbance $\hat{\boldsymbol{u}}$, the rotation rate, $\dot{\boldsymbol{p}}$, and fibre distribution $g(\boldsymbol{p})$. In deriving (37) we assumed that non-Newtonian effects are negligible, and that the rotation rate of the fibres is approximately equal to the Jeffery rotation rate.

In Jeffery orbits, fibres of high aspect ratio ($r \gg 1$) spend nearly all of their orbit in alignments approximately perpendicular to the gradient direction, and at any one time only an $O(1/r)$ fraction of the fibres are in orientations with $|p_2|$ greater than $1/r$. The velocity disturbance caused by an aligned fibre is smaller by a factor of $1/r^2$ from that caused by a fibre with p_2 of order unity. Thus, the dominant contribution to the integral comes from the $1/r$ fraction of fibres with p_2 of order unity. We will therefore only consider interactions with fibres with $|p_2| \gg 1/r$.

We introduce polar coordinates in which θ is the angle between the fibre and the flow direction (1) and ϕ is the angle between the gradient direction (2) and the projection of the fibre in the gradient, vorticity (2, 3)-plane. This is the coordinate system used by Koch & Shaqfeh (1990), but differs from that used by Jeffery (1922). In this coordinate system the rotation rate of a fibre with $|\theta| \gg 1/r$ at leading order in $1/r$, is

$$\dot{\theta} = -\sin^2\theta\cos\phi, \quad \dot{\phi} = 0, \tag{40}$$

so that ϕ remains constant along an orbit, and θ varies with ζ as

$$\cot\theta = \cot\theta_0 - \frac{(\zeta - k_2)}{k_1}\cos\phi, \tag{41}$$

where θ_0 is the angle of the fibre at $\zeta = k_2$, and

$$\hat{\omega}(\zeta) = -\sin^3\theta\cos\phi. \tag{42}$$

From Jeffery's solution, the fibre orientation distribution, $g(\boldsymbol{p})$ must be of the form

$$g(\boldsymbol{p}) = \frac{1}{r\sin^2\theta}T(\phi). \tag{43}$$

The function $T(\phi)$ depends on the distribution of fibres between Jeffery orbits. In general, this distribution will be affected by both interactions between the fibres and non-Newtonian effects. The non-Newtonian drift between Jeffery orbits is calculated in §3, but in the present calculation we consider the case when the polymer concentration is sufficiently low that $T(\phi)$ is determined solely by fibre interactions. In

this case we can use the experimental measurements of Anczurowski & Mason (1967) for fibres of aspect ratio 18.4 suspended in a Newtonian fluid, which have recently been fitted with a calculation based on a weak anisotropic rotary diffusivity (Stover, Koch & Cohen 1992), for which

$$T(\phi) = \frac{S}{\pi[4S\cos^2\phi + \sin^2\phi]^{\frac{3}{2}}}. \tag{44}$$

The best fit is obtained for $S = 17$.

In a dilute fibre suspension, the velocity disturbances generated by the fibres are uncorrelated at leading order in nl^3, and so the conditionally averaged velocity disturbance, $\langle \boldsymbol{u}^f \rangle_1$, can be approximated as the velocity disturbance generated by an isolated fibre in shear flow. This approximation produces errors of order $nl^3/\log(r)$ in $\langle \boldsymbol{u}^f \rangle_1$. The velocity disturbance at the origin produced by a fibre at position $\boldsymbol{x}$ is given by slender-body theory (Batchelor 1970) as

$$\langle \boldsymbol{u}' \rangle = \int_{-1}^{1} \mathrm{d}\lambda \boldsymbol{J}(\boldsymbol{x} + \lambda \boldsymbol{p}) \cdot \boldsymbol{f}(\lambda), \tag{45}$$

where

$$\boldsymbol{J}(\boldsymbol{x}) = \frac{1}{8\pi}\left(\frac{\boldsymbol{I}}{|\boldsymbol{x}|} + \frac{\boldsymbol{x}\boldsymbol{x}}{|\boldsymbol{x}|^3}\right)$$

is the Oseen tensor and

$$\boldsymbol{f}(\lambda) = -\frac{2\pi}{\log(r)} p_1 p_2 \lambda \boldsymbol{p}$$

is the force per unit length exerted by the fibre on the flow. Taking the Fourier transform of (45) and using the results

$$\int_{-1}^{1} \lambda \, \mathrm{e}^{\mathrm{i}\lambda \boldsymbol{k}\cdot\boldsymbol{p}} \mathrm{d}\lambda = 2\mathrm{i} j_1(\boldsymbol{k}\cdot\boldsymbol{p}), \tag{46}$$

$$\int \mathrm{d}^3\boldsymbol{x} \boldsymbol{J}(\boldsymbol{x}) \, \mathrm{e}^{-\mathrm{i}\boldsymbol{k}\cdot\boldsymbol{x}} = \frac{1}{k^2}\left(\boldsymbol{I} - \frac{\boldsymbol{k}\boldsymbol{k}}{k^2}\right), \tag{47}$$

we find that $\hat{\boldsymbol{u}}$ is given by

$$\hat{\boldsymbol{u}} = -\frac{4\pi \mathrm{i} p_1 p_2}{\log(r)}\left(\frac{\boldsymbol{p}}{k^2} - \frac{(\boldsymbol{k}\cdot\boldsymbol{p})\boldsymbol{k}}{k^4}\right) j_1(\boldsymbol{k}\cdot\boldsymbol{p}). \tag{48}$$

In (46) and (47), $j_1 \equiv (\sin x)/x^2 - (\cos x)/x$ is the first-order spherical Bessel function.

Since $\hat{\boldsymbol{u}}$ is antisymmetric in $\boldsymbol{k}$, we can use the symmetry of the integrand in $\boldsymbol{k}$ to write

$$M_{ijkl} = -\frac{1}{8\pi^3 r}\int_0^{2\pi} \mathrm{d}\phi \, T(\phi) \int_0^{\pi} \mathrm{d}\theta_0 \frac{1}{\sin^2\theta_0} \int \mathrm{d}^3\boldsymbol{k} \frac{k_j \hat{u}_i}{|k_1|} \int_{-\infty}^{k_2} \mathrm{d}\zeta \, k_l \hat{u}_k. \tag{49}$$

In the special case when $i = k$ and $j = l$ the streamline integration may be performed by parts to give (no summation over i and j)

$$M_{ijij} = -\frac{1}{16\pi^3 r}\int_0^{2\pi} \mathrm{d}\phi \, T(\phi) \int_0^{\pi} \mathrm{d}\theta_0 \frac{1}{\sin^2\theta_0} \int_{-\infty}^{\infty} \mathrm{d}k_1 \frac{1}{|k_1|} \int_{-\infty}^{\infty} \mathrm{d}k_3 \left[\int_{-\infty}^{\infty} \mathrm{d}k_2 \, k_j \hat{u}_i\right]^2. \tag{50}$$

As discussed earlier (§2.2), M_{2121} is of order $1/r\log^2 r$, and integrating, (50) numerically using the expression for $T(\phi)$ given in (44) we obtain

$$M_{2121} = 0.038\ldots \times 1/r\log^2 r \tag{51}$$

and
$$M_{3131} = 0.12\ldots \times 1/r\log^2 r, \tag{52}$$

and therefore D_{crit} is equal to

$$D_{\text{crit}} = 3.7 \times \left(\frac{nl^3}{r\log^2 r}\right)^{-\frac{1}{3}}. \tag{53}$$

It should be noted that the numerical value obtained for M_{2121} depends critically upon the expression for $T(\phi)$, which varies with the concentration of fibres and polymers. In consequence the numerical value should be treated with caution. However, it is clear that a large Deborah number is required to produce a significant change in the extension of the polymer in a truly dilute suspension, because the frequency of interactions between rotating fibres and polymers is low. We would expect to find lower values of the critical Deborah number for more concentrated suspension, where the frequency of interactions is higher.

2.6. *Semi-dilute suspensions*

A concentration of fibres for which nl^3 is large compared to unity, but small compared to r is referred to as semi-dilute. In shear flow, the fibres continue to rotate in approximate Jeffery orbits (see Stover *et al.* 1992; Koch & Shaqfeh 1990), and therefore the number of density of fibres with p_2 greater than order $1/r$ remains nl^3/r, which is small. Hence, the concentration of rotating fibres is dilute and we may continue to use the dilute approximations for the rotating fibres for $nl^3 \ll r$. However, the conditionally averaged velocity $\langle \boldsymbol{u}^{\text{f}} \rangle_1$ is no longer equal to the velocity of an isolated fibre in shear flow, because of the presence of fibres aligned in the flow direction. The orientation distribution of the fibres is determined by interactions between fibres and these are also different in this concentration regime. Thus M_{ijkl} remains given by (49), but with different expression for $\hat{\boldsymbol{u}}$ and $T(\phi)$.

In experiments with semi-dilute suspensions of fibres in Newtonian fluids Stover *et al.* (1992) found that the distribution of fibres between Jeffery orbits may still be approximated by (44), but using much smaller values of S than for dilute suspensions. Stover *et al.* obtained a best fit for fibres of aspect ratio 31.9 with S equal to 2 for values of nl^3 between 0.6 and 6. The fact that S is smaller for a semi-dilute suspension than a dilute suspension indicates that a greater proportion of the fibres are in orbits near the 1, 2 (flow, gradient)-plane, which should increase the effect of the fibres on the polymer.

The velocity disturbance can be found from the ensemble-averaged Green's function for a semi-dilute suspension of aligned fibres derived by Shaqfeh & Fredrickson (1990). The component of $\hat{\boldsymbol{u}}$ needed to calculate M_{2121} *is* $\hat{u}_2$, given by

$$\hat{u}_2 = -\frac{4\pi i p_1 p_2}{\log(rX)}\frac{k^2}{k^2-\alpha_2}\left(\frac{p_2}{k^2}+\beta_1\frac{k_2\boldsymbol{k}\cdot\boldsymbol{p}}{k^2}+\beta_2\frac{k_2 p_1}{k}\right)j_1(\boldsymbol{k}\cdot\boldsymbol{p}), \tag{54}$$

where

$$\beta_1 = -\frac{1}{k^2}\left(\frac{k^2-\alpha_1}{k^2-\alpha_1+(\alpha_1-\alpha_2)k_1^2/k^2}\right),$$

$$\beta_2 = \frac{1}{k^2}\left(\frac{(\alpha_2-\alpha_1)k_1 k}{k_1^2(k^2-\alpha_2)+(k^2-k_1^2)(k^2-\alpha_1)}\right),$$

$$\alpha_1 = \frac{4\pi nl^3}{\log(rX)}[j_0^2(k_1)-1], \quad \alpha_2 = \frac{8\pi nl^3}{\log(rX)}[3j_1^2(k_1)+j_0^2(k_1)-1]$$

and $j_0(x) \equiv \sin x/x$ is the spherical Bessel function of order zero. The screening length X is defined implicitly by

$$X^2 = \log(rX)/8\pi nl^3.$$

The dominant contribution to the integral for M_{2121} ((50) with $\hat{u}_2$ given by (54)) comes from wavenumbers of order $1/X$, suggesting that M_{2121} should be proportional to $X/r\log^2(rX)$. Integrating the expression for M_{2121} numerically for different values of nl^3 we find that there is a logarithmic correction to this scaling, with

$$M_{2121} \sim 0.069\ldots\left(\frac{X\log(1/2X^2)}{r\log^2(rX)}\right) \quad \text{for} \quad 1 \ll nl^3 \ll r, \tag{55}$$

giving a value for the critical Deborah number of

$$D_{\text{crit}} \sim 4.6\times\left(\frac{r^2\log^3(rX)}{nl^3\log^2(1/2X^2)}\right)^{\frac{1}{6}}. \tag{56}$$

Thus the critical Deborah number continues to decrease with increasing concentration throughout the semi-dilute regime. However, the dependence on the fibre concentration drops from $(nl^3)^{\frac{1}{3}}$ for a dilute suspension to $(nl^3)^{\frac{1}{6}}$ due to the screening of the velocity disturbance by the other fibres in the suspension.

2.7. *Discussion*

The preceding analysis suggests that at shear rates above some critical value the polymers become significantly more extended in a fibre suspension than in polymer solution alone. To date, however, we know of no experimental evidence for this phenomenon. The most direct way to measure the extension of the polymer would be to measure the birefringence, but we know of no experiments of this kind on sheared suspensions of fibres.

There should also be an associated rise in shear viscosity with shear rate as given by (35). However, this may be difficult to detect in practice for the following reasons. First, our analysis neglects the non-Newtonian nature of the fluid and is, therefore, strictly applicable only to very dilute polymer solutions where the polymer stress is small. Viscosity measurements of fibres suspended in polymer melts and concentrated solutions, which are strongly shear-thinning, find that the viscosity becomes less dependent on fibre concentration as the shear rate increases (see the review by Ganani & Powell 1985, and Kitano *et al.* 1988), presumably as a consequence of the localization of the fibre disturbance due to shear-thinning. For this reason, an increase in viscosity may be detectable only in Boger fluids (Boger 1977), which have constant shear viscosities. Second, the orientation distribution of fibres is expected to vary with shear rate and polymer concentration and this will affect the magnitude of the parameter M_{2121}. There are no simultaneous measurements of shear viscosity and orientation distribution. For these reasons birefringence may be the best method for detecting this phenomenon.

3. The effect of the polymer on the fibre motion

In this section we consider the affect of the polymer stress on the motion of the fibres. The rotational velocity, $\dot{\boldsymbol{p}}$, of each individual fibre within a suspension in a dilute polymer solution may be written as the sum of three terms

$$\dot{\boldsymbol{p}} = \dot{\boldsymbol{p}}^{\mathrm{J}} + \dot{\boldsymbol{p}}^{\mathrm{p}} + \dot{\boldsymbol{p}}^{\mathrm{f}};$$

$\dot{\boldsymbol{p}}^{\mathrm{J}}$ is the Jeffery rotation rate for a fibre in shear flow, $\dot{\boldsymbol{p}}^{\mathrm{p}}$ is the perturbation caused by the polymer, and $\dot{\boldsymbol{p}}^{\mathrm{f}}$ is the perturbation caused by the presence of other fibres. The calculations in the previous section assumed that $|\dot{\boldsymbol{p}}^{\mathrm{p}}| \ll |\dot{\boldsymbol{p}}^{\mathrm{f}}| \ll |\dot{\boldsymbol{p}}^{\mathrm{J}}|$, so that $\dot{\boldsymbol{p}}$ was approximately equal to $\dot{\boldsymbol{p}}^{\mathrm{J}}$ and $T(\phi)$ was determined by $\dot{\boldsymbol{p}}^{\mathrm{f}}$. In this section we calculate $\dot{\boldsymbol{p}}^{\mathrm{p}}$ and determine its effect on the fibre motion.

We assume that $\dot{\boldsymbol{p}}^{\mathrm{p}}$ and $\dot{\boldsymbol{p}}^{\mathrm{f}}$ are small in comparison to $\dot{\boldsymbol{p}}^{\mathrm{J}}$ so that fibres rotate in approximate Jeffery orbits. From slender-body theory, $\dot{\boldsymbol{p}}^{\mathrm{p}}$ for a fibre at the origin is given by

$$\dot{\boldsymbol{p}}^{\mathrm{p}} = \frac{3}{2}\int_{-1}^{1} (\boldsymbol{I}-\boldsymbol{pp})\,\boldsymbol{u}^{\mathrm{p}}(\lambda \boldsymbol{p})\,\lambda\,\mathrm{d}\lambda, \tag{57}$$

where $\boldsymbol{u}^{\mathrm{p}}$ is the velocity disturbance caused by the polymer. In this limit where the non-Newtonian stresses are small compared to the Newtonian stresses, we can calculate $\boldsymbol{u}^{\mathrm{p}}$ from a perturbation expansion, so that at leading order $\boldsymbol{u}^{\mathrm{p}}(\boldsymbol{x})$ is given by

$$\boldsymbol{u}^{\mathrm{p}}(\boldsymbol{x}) = \int \mathrm{d}^3\boldsymbol{x}'\boldsymbol{J}(\boldsymbol{x}-\boldsymbol{x}')\boldsymbol{f}^{\mathrm{p}}(\boldsymbol{x}'), \tag{58}$$

where $\boldsymbol{f}^{\mathrm{p}}(\boldsymbol{x})$ is the divergence of the polymeric stress at position $\boldsymbol{x}'$ based on the Newtonian velocity of a fibre in shear flow. For a solution of linear dumbbells, $\boldsymbol{f}^{\mathrm{p}}$ is given by

$$\boldsymbol{f}^{\mathrm{p}} = (2c/D)\,\nabla\cdot\boldsymbol{A} \tag{59}$$

and results from gradients in the extension of the dumbbells and does not depend on its mean value. Consequently, it is useful to split $\boldsymbol{A}$ and the velocity $\boldsymbol{u}$ as the sum of their average values plus the perturbation caused by the fibre

$$\boldsymbol{A} = \langle \boldsymbol{A}\rangle_0 + \boldsymbol{A}^{\mathrm{f}}, \quad \boldsymbol{u} = \boldsymbol{u}_0 + \boldsymbol{u}^{\mathrm{f}}. \tag{60}$$

The perturbations are of order $1/\log(r)$ smaller than the average values, and at high Deborah numbers the relaxation time is large compared to the time taken for a polymer to pass the fibre. Neglecting terms of order $1/\log^2(r)$ and $1/D\log(r)$, the evolution of $\boldsymbol{A}^{\mathrm{f}}$ is approximately given by

$$(\mathrm{D}/\mathrm{D}t)\,\boldsymbol{A}^{\mathrm{f}} = \langle \boldsymbol{A}\rangle_0\cdot\nabla\boldsymbol{u}^{\mathrm{f}} + (\nabla\boldsymbol{u}^{\mathrm{f}})^{\mathrm{T}}\cdot\langle \boldsymbol{A}\rangle_0. \tag{61}$$

In view of the convolution integrals in (57) and (58), it proves easier to work in transform space. Taking the Fourier transform of (61) we obtain

$$\hat{\boldsymbol{A}}^{\mathrm{f}} = -\mathrm{i}\int_{\infty\mathrm{sgn}(k_1)}^{k_2} \frac{1}{k_1}(\langle \boldsymbol{A}\rangle_0\cdot\boldsymbol{k}\hat{\boldsymbol{u}} + \hat{\boldsymbol{u}}\boldsymbol{k}\cdot\langle \boldsymbol{A}\rangle_0)\,\mathrm{d}k_2, \tag{62}$$

where $\hat{\boldsymbol{u}}$ is the Fourier transform of $\boldsymbol{u}^{\mathrm{f}}$, given (from (48)) by

$$\hat{u} = \frac{4\pi\mathrm{i}p_1p_2}{\log(r)}\left(\frac{\boldsymbol{p}}{k^2} - \frac{(\boldsymbol{k}\cdot\boldsymbol{p})\,\boldsymbol{k}}{k^4}\right) j_1(\boldsymbol{k}\cdot\boldsymbol{p}). \tag{63}$$

The change in sign is because the fibre rather than the polymer is now at the origin.

Taking the Fourier transforms of (57), (58) and (59) we find

$$\hat{p}_i = \frac{6c}{Dk^2} j_1(\boldsymbol{k}\cdot\boldsymbol{p})(\delta_{ij}-p_ip_j)\left(\delta_{jk}-\frac{k_jk_k}{k^2}\right)k_l\hat{A}^{\mathrm{f}}_{kl}, \tag{64}$$

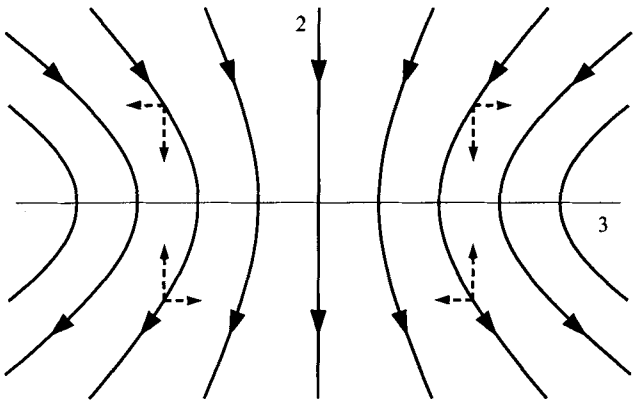

FIGURE 6. Sketch of Jeffery orbits near the flow direction. Dashed lines indicate the direction of $\dot{\boldsymbol{p}}^{\mathrm{p}}$.

and the rotation rate of a fibre at the origin $\dot{\boldsymbol{p}}^{\mathrm{p}}$ is given by

$$\dot{\boldsymbol{p}}^{\mathrm{p}} = \frac{1}{8\pi^3}\int \mathrm{d}^3\boldsymbol{k}\hat{\boldsymbol{p}}. \tag{65}$$

From (62)–(65), the additional angular velocity $\dot{\boldsymbol{p}}^{\mathrm{p}}$ may be written in the form

$$\dot{p}_i^{\mathrm{p}} = \frac{c}{D\log(r)} B_{ijk}(\boldsymbol{p})\langle A_{jk}\rangle_0, \tag{66}$$

where $B_{ijk}(\boldsymbol{p})$ is a four-dimensional integral. This expression for $\dot{\boldsymbol{p}}^{\mathrm{p}}$ neglects terms that are of relative order $1/\log(r)$ and $1/D$ smaller from the approximation of $\boldsymbol{A}^{\mathrm{f}}$ in (61). There are also errors of relative order $c|\langle \boldsymbol{A}\rangle_0|/D$ from neglecting the polymeric stress in $\boldsymbol{u}^{\mathrm{f}}$.

The value of B_{ijk} may be calculated numerically for all fibre orientations. However, if $\dot{\boldsymbol{p}}^{\mathrm{p}}$ is small the most easily measured consequences of this perturbation come from its average effect over a large number of orbits. As noted previously, the fibres spend almost all their time in orientations perpendicular to the gradient direction, and only for an order $1/r$ fraction of time is $|p_2| > 1/r$. Additionally, all Jeffery orbits pass within an angle of order $1/r$ of the flow direction and so a small drift in angle at this orientation will produce a large change in the subsequent motion of the fibre. For these reasons we expect the most significant effects of the polymer on the orientation of the fibre to occur when p_2 is small.

3.1. *Fibre rotation when p_2 is small*

If p_2 is small, the rotation rate of the fibre will be small compared to the shear rate, and so a fibre will not rotate in the time it takes a polymer to pass. This greatly simplifies the calculation of $\dot{\boldsymbol{p}}^{\mathrm{p}}$ and analytic progress is possible. In this limit the velocity disturbance caused by the fibre will be linear in p_2, and consequently $\dot{\boldsymbol{p}}^{\mathrm{p}}$ will be linear p_2.

The path of a Jeffery orbit is symmetric in p_2 (see figure 6), and therefore any cumulative drift in orbit must come from the 2-component, $\dot{p}_2^{\mathrm{p}}$. As a consequence of the flow symmetry, we find that the only non-zero contribution to this component is proportional to $\langle A_{22}\rangle_0$. In this limit the expression for $\dot{p}_2^{\mathrm{p}}$ may be greatly simplified by elementary algebraic manipulations. At leading order, k_1, k_3 and $\boldsymbol{k}\cdot\boldsymbol{p}$ are independent of k_2, and so the k_2 integrations in (62) and (65) may be performed analytically. The

remaining integrals over k_1 and k_3 can be simplified by changing coordinates to $z = \boldsymbol{k}\cdot\boldsymbol{p}$ and $\eta = \cos^{-1}[\boldsymbol{k}\cdot\boldsymbol{p}/(k_1^2+k_3^2)^{\frac{1}{2}}]$. The η-integration can be performed analytically leaving a single integral over z:

$$\dot{p}_2^{\mathrm{p}} = -\frac{6cp_1p_2\langle A_{22}\rangle_0}{\pi D\log r}\left(\int_0^\infty j_1^2(z)\,\mathrm{d}z\right)\log\left(\frac{1+p_1}{p_3}\right). \tag{67}$$

Thus the additional rotation of the fibres caused by the polymer is towards the 1,3 (flow, vorticity)-plane. From the direction of the Jeffery orbits shown in figure 6 it can be seen that this will cause the fibres to drift to orbits away from the 1,2 (flow, gradient)-plane and towards the vorticity axis. In the limit when p_2 and p_3 are small compared to $1/r$, the logarithm is cut off by the finite aspect ratio of the fibre.

For alignments close to the flow direction, the Jeffery rotation rate is approximately

$$\dot{p}_2^J = -p_2^2 - 1/r^2, \quad \dot{p}_3^{\mathrm{J}} = -p_2p_3, \tag{68}$$

with solution

$$p_2 = -\frac{1}{r}\tan\left[\frac{(t-t_0)}{r}\right], \quad p_3 = \frac{1}{rC}\sec\left[\frac{(t-t_0)}{r}\right], \tag{69}$$

where C is the Jeffery orbit constant (Leal 1975), which varies from 0 (a fibre aligned with the vorticity axis) to infinity (a fibre rotating in the (1,2)-plane).

From (67) the perturbation to $\dot{p}_2$, is of the form

$$\dot{p}_2^{\mathrm{p}} = -2\kappa p_2, \tag{70}$$

where κ is positive and approximately constant,

$$\kappa \approx \frac{3c\langle A_{22}\rangle_0}{\pi D}\left(\int_0^\infty j_1^2(z)\,\mathrm{d}z\right) = 0.5\times\frac{c\langle A_{22}\rangle_0}{D}. \tag{71}$$

The leading-order contribution to $\dot{p}_3^{\mathrm{p}}$ comes from the 12-component of $\langle\boldsymbol{A}\rangle_0$, and is of order $p_2p_3\log(1/|p_2|)\log(1/|p_3|)$. Unfortunately, $\dot{p}_3^{\mathrm{p}}$ cannot be simplified in the same manner as $\dot{p}_2^{\mathrm{p}}$ because the k_2-integration cannot performed analytically. However, it is possible to show that $\dot{p}_3^{\mathrm{p}}$ has the form

$$\dot{p}_3^{\mathrm{p}} = Kp_2p_3, \tag{72}$$

where K is positive and

$$K = O\left(\frac{c\langle A_{12}\rangle_0\log(1/p_3)\log(1/p_2)}{D\log(r)}\right).$$

Thus for p_2 and p_3 of order $1/r$, $\dot{p}_3^{\mathrm{p}}$ is of order K/r^2 and is small in comparison to $\dot{p}_2^{\mathrm{p}}$ provided $K/\kappa \ll r$.

The effect of including $\dot{p}_2^{\mathrm{p}}$ is to change the Jeffery orbit (69) to

$$p_2 = -\frac{b}{r}\left\{\tan\left[\frac{(t-t_0)\,b}{r}\right]+\kappa\right\}, \quad p_3 = \frac{b}{rC\,\mathrm{e}^{-\kappa bt}}\sec\left[\frac{(t-t_0)\,b}{r}\right], \tag{73}$$

where $b = (1-\kappa^2r^2)^{\frac{1}{2}}$. Thus the perturbation to $\dot{p}_2$ has two effects. First, the orbit constant decrease by a factor of $\exp(-\kappa\pi)$ over half an orbit, so that the fibre drifts towards the vorticity axis. Second, the period of rotation increases by a factor of $1/b$. For κ greater than $1/r$ the fibre no longer rotates at all in the (1,2)-plane. Instead p_2 tends to a constant negative value, p_2^0,

$$p_2^0 \equiv -\kappa + (\kappa^2 - 1/r^2)^{\frac{1}{2}}, \tag{74}$$

and p_3 increases exponentially, so that the fibre will rotate towards the vorticity axis. The point $p_2 = p_2^0$, $p_3 = 0$ is now a position of equilibrium, but it is unstable to perturbations in p_3.

3.2. *Discussion*

The approximations used in deriving the results for this section are valid for high Deborah numbers when the polymer responds affinely to the velocity disturbance caused by the fibre. The opposite limit of small Deborah number is analysed by Leal (1975) using a second-order-fluid model. For small angles away from the (1, 3)-plane these two different theories predict qualitatively similar behaviour. However, the mechanisms which give rise to the non-Newtonian perturbations are quite different. The similarity in the motion generated by these two different mechanisms occurs because in both cases the induced angular velocity is linear in the disturbance velocity, and hence linear in p_2.

Detailed experimental observations of the motion of fibres suspended in aqueous poly-acrylamide have been made by Bartram *et al.* (1975). They observe that fibres drift towards the vorticity axis and that the period of rotation is considerably longer than in a Newtonian fluid, in qualitative agreement with both Leal's analysis and our small-angle theory. The second-order fluid model requires the existence of a second-normal-stress difference to produce a perturbation to the fibre rotation rate. Typically, the second-normal-stress difference of a polymer solution is about one tenth of the first-normal-stress difference. However, Iso *et al.* (1993) observe that fibres also drift towards the vorticity axis in polyisobutylene-based Boger fluids, even though these fluids have no second-normal-stress difference (Magda *et al.* 1991). In our anaylsis for small angles we find that the drift is proportional to $c\langle A_{22}\rangle_0/D$. In shear flow (without fibres) $\langle A_{22}\rangle_0$ is constant for linear dumbbells and so the magnitude of this effect would decrease with Deborah number. However, in §2 we found that the presence of fibres will cause $\langle A_{22}\rangle_0$ to increase with Deborah number (equation (27)).

Above a critical shear rate Bartram *et al.* observe that a fibre placed in the (1, 2)-plane rotates towards the flow direction and subsequently remains aligned in approximately the flow direction until disturbed by a second fibre. Both Leal's and our small-angle theory predict that above a critical value of the relevant non-Newtonian parameter, in our case κ, a fibre rotating in the (1, 2)-plane will cease to rotate. However, the position $p_3 = 0$, $p_2 = p_2^0$ is unstable to motion in the p_3 direction. From (68), the time taken for the fibre to drift away from this position is of order $1/|p_2^0|$ (which is of order r), and so is of the same order as the period of a Jeffery orbit. Thus neither theory is able to explain this observation of permanent alignment within the parameter range for which they are valid. Our theory would predict a stable fixed point if K is permitted to be greater than unity, whereas the equivalent term for a second-order fluid is destabilizing.

More recently, Stover & Cohen (1990) compared the drift between Jeffery orbits for fibres suspended in a polyacrylamide/water/glycerine mixture with Leal's theory. By choosing the value of the second-normal-stress difference that provided the best fit, they found good agreement between experiment and theory. However, they did not measure the second-normal-stress difference independently to compare the true value with the value that gives the best fit. Our theory could also account for the drift seen in these experiments, but does not depend on the second-normal-stress difference.

Johnson, Salem & Fuller (1990) used optical dichroism to study the orientation of suspensions of hematite particles in Boger fluids. The particles were spheroidal in shape with aspect ratios between 2.7 and 5.8. For the smallest-aspect-ratio particles ($r = 2.7$), the mean direction of orientation in the (1, 2)-plane was at a small angle to the flow

direction with $p_2 < 0$. This is consistent with the perturbation to $\dot{p}_2$ given by (67). They also studied the motion of these particles in concentrated solutions of monodisperse polystyrene. The mean direction of alignment of the particles corresponds to $p_2 \approx 0.25$, at odds with both theory and the Boger fluid experiments.

The drift of the fibres towards the vorticity axis has important implications for the calculations performed in §2. If a large majority of the fibres are in orbits close to the vorticity axis the magnitude of the flow disturbance and consequently of M_{2121} will be smaller. However, it is expected that fibre–fibre interactions will prevent the fibres from becoming completely aligned with the vorticity axis. This is supported by experimental measurements of the orientation distribution by Gauthier, Goldsmith & Mason (1971) who find that the distribution is shifted towards the vorticity axis compared to a Newtonian fluid, but that a proportion of the fibres remain in orbits away from the vorticity axis. In recent experiments with semi-dilute suspensions of fibres in a Boger fluid, Iso *et al.* (1993) find that the orientation distribution of a 0.01 % polyacrylamide solution is indistinguishable from that for a Newtonian fluid at the same fibre concentration. Fibre–fibre interactions are stronger in a semi-dilute suspension and appear to dominate non-Newtonian effects at this concentration. Thus, we would still expect to see an increase in extension, but the critical Deborah number may be somewhat larger at higher polymer concentrations.

This work was mostly carried out while O. G. H. was a post-doctoral research fellow at Cornell University, and was supported by the US Army Research Office through the Mathematical Sciences Institute of Cornell University, and by the Cornell Injection Molding Program Consortium. The authors also gratefully acknowledge financial support from the Hoechst Celanese Corporation and the Embiricos Foundation at Jesus College, Cambridge.

REFERENCES

ANCZUROWSKI, E. & MASON, S. G. 1967 Kinetics of flowing dispersions III. Equilibrium orientations of rods and discs. *J. Colloid Interface Sci.* **23**, 533.

BARTRAM, E., GOLDSMITH, H. L. & MASON, S. G. 1975 Particle motions in non-Newtonian media III. Further observations in elasticoviscous fluids. *Rheol. Acta* **14**, 776.

BATCHELOR, G. K. 1970 Slender body theory for particles of arbitrary cross-section in Stokes flow. *J. Fluid Mech.* **44**, 419.

BOGER, D. V. 1977 A highly-elastic constant-viscosity fluid. *J. Non-Newtonian Fluid Mech.* **3**, 87.

FRATTINI, P. L., SHAQFEH, E. S. G., LEVY, J. L. & KOCH, D. L. 1991 Observations of axisymmetric tracer particle orientation during flow through a dilute fixed bed of fibres. *Phys. Fluids* A **3**, 2516.

GANANI, E. & POWELL, R. L. 1985 Suspensions of rodlike particles: literature review and data correlations. *J. Composite Mater.* **19**, 195.

GAUTHIER, F., GOLDSMITH, H. L. & MASON, S. G. 1971 The kinetics of flowing dispersions V. Orientation distributions of cylinders in Newtonian and non-Newtonian systems. *Kolloid-Z. Z. Polymere* **248**, 1000.

ISO, Y., KOCH, D. L. & COHEN, C. 1993 Orientation of fibers in non-Newtonian fluids subject to simple shear. (in preparation).

JAMES, D. F. & MCCLAREN, D. R. 1975 The laminar flow of dilute polymer solutions through a porous media. *J. Fluid Mech.* **70**, 733.

JEFFERY, G. B. 1922 The motion of ellipsoidal particles immersed in a viscous fluid. *Proc. R. Soc. Lond.* A **102**, 161.

JOHNSON, S. J., SALEM, A. J. & FULLER, G. G. 1990 Dynamics of colloidal particles in sheared non-Newtonian fluids. *J. Non-Newtonian Fluid Mech.* **34**, 89.

KITANO, T., FUNABASHI, M., KLASON, C. & KUBAT, J. 1988 Shear flow properties of carbon fibre-filled polyethylene melts. *Intl Polym. Proc.* III **2**, 67.

KOCH, D. L. & SHAQFEH, E. S. G. 1990 The average rotation rate of a fiber in the linear flow of a semidilute suspension. *Phys. Fluids* A **2**, 2093.

KUHN, W. & KUHN, H. 1945 Bedeutung beschränkt freir drehbarkeit für die Viskosität und Strömungsdoppelbrechung von Fadenmolekellosungen. I. *Helv. Chim. Acta* **28**, 1533.

LEAL, L. G. 1975 The slow motion of slender rod-like particles in a second order fluid. *J. Fluid Mech.* **69**, 305.

MAGDA, J. J., LOU, J., BAEK, S.-G. & DEVRIES, K. L. 1991 Second normal stress difference of a Boger fluid. *Polymer* **32**, 2000.

PETERLIN, A. 1966 Hydrodynamics of macromolecules in a velocity field with longitudinal gradient. *J. Polym. Sci.* **4**, 287.

RALLISON, J. M. & HINCH, E. J. 1988 Do we understand the physics in the constitutive equation? *J. Non-Newtonian Fluid Mech.* **29**, 37.

SHAQFEH, E. S. G. & FREDRICKSON, G. H. 1990 The hydrodynamic stress in a suspension of rods. *Phys. Fluids* A **2**, 7.

SHAQFEH, E. S. G. & KOCH, D. L. 1988*a* The effect of hydrodynamic interactions on the orientation of axisymmetric particles flowing through a fixed bed of spheres or fibers. *Phys. Fluids* **31**, 728.

SHAQFEH, E. S. G. & KOCH, D. L. 1988 *b* The combined effects of hydrodynamic interactions and Brownian motion on the orientation of particles flowing through fixed beds. *Phys. Fluids* **31**, 2769.

SHAQFEH, E. S. G. & KOCH, D. L. 1990 Orientational dispersion of fibers in extensional flows. *Phys. Fluids* A **2**, 1077.

SHAQFEH, E. S. G. & KOCH, D. L. 1992 Polymer stretch in dilute fixed beds of fibres or spheres. *J. Fluid Mech.* **244**, 17.

STOVER, C. A. & COHEN, C. 1990 The motion of rod-like particles in the pressure driven flow between two flat plates. *Rheol. Acta* **29**, 203.

STOVER, C. A., KOCH, D. L. & COHEN, C. 1992 Observations of fibre orientation in simple shear flows of semi-dilute suspensions. *J. Fluid Mech.* **238**, 277.

WARNER, H. R. 1972 Kinetic theory and rheology of finitely extensible dumbbells. *Ind. Engng Chem. Fundam.* **20**, 227.